JOURNAL OF CULTURAL ANALYSIS AND SOCIAL CHANGE

Journal of Cultural Analysis and Social Change,
2025, 10(4), 3994-4012
ISSN: 2589-1316

Green-Synthesized Gold Nanoparticles from Centella asiatica for Colloidal Stability and UV Protection

Mingle A Pistanty[1], Okid Parama Astirin[2]*, Soerya Dewi Marliyana[3], Solichatun[4]

[1] *Department of Biology, Universitas Sebelas Maret, Surakarta, INDONESIA, Email: mingle@fkip.uncen.ac.id, https://orcid.org/0000-0002-1288-9658*
[2] *Department of Biology, Universitas Sebelas Maret, Surakarta, INDONESIA, Email: parama_astirin@staff.uns.ac.id, https://orcid.org/0009-0002-8327-4711*
[3] *Department of Chemistry, Universitas Sebelas Maret, Surakarta, INDONESIA; https://orcid.org/0000-0001-9722-3590*
[4] *Department of Biology, Universitas Sebelas Maret, Surakarta, INDONESIA; https://orcid.org/0000-0002-6566-3636*

*__Corresponding Author:__ mingle@fkip.uncen.ac.id

Citation: Pistanty, M. A., Astirin, O. P., Marliyana, S. W., & Solichatun, (2025). Green-Synthesized Gold Nanoparticles from Centella asiatica for Colloidal Stability and UV Protection, *Journal of Cultural Analysis and Social Change*, 10(4), 3994-4012. https://doi.org/10.64753/jcasc.v10i4.3716

Published: December 27, 2025

ABSTRACT

Green synthesized gold nanoparticles (AuNPs) using Centella asiatica leaf extract and the influence of poly(vinyl alcohol) (PVA) as a respective secondary stabilizing agent were systematically studied. Formation of AuNP was verified by a color change and absorption peaks due to the surface plasmon resonance in the visible region. Several characterization techniques such as UV–Vis-spectrophotometry, particle size analysis and zeta potential measurement, scanning electron microscopy, Fourier transform infrared spectroscopy (FT-IR), and energy-dispersive X-ray (EDX) were employed. The PVA content dramatically affected the growth and dispersion of nanoparticles. The PVA-containing systems showed a larger hydrodynamic size and polydispersity, which implied competitive adsorption among phytochemicals and with PVA as well as polymer-bridging effects. In spite of the size increase, zeta potential and conductimetric measurements showed that colloidal stability was increasing as a result of steric stabilization. The FTIR and EDX studies confirmed a co-capping mode where the plant-based biomolecules remained attached on the AuNP surface along with adsorbed PVA. Functional testing using Sun Protection Factor (SPF) measurements showed the opposite trend; for all AuNP formulations without PVA, higher SPF values were measured that peaked at intermediate storage times. This observation indicates the existence of an optimal functional window where ordered aggregation improves UV scattering performance. Overall, the results underscore a non-monotonic relationship between colloidal stability and functionality in plant-mediated AuNP systems and the importance of tuning these parameters when designing sustainably nanoparticle-based materials.

Keywords: Centella Asiatica, Green Synthesis, Gold Nanoparticles, Poly(Vinyl Alcohol), Optical Stability, UV Protection.

INTRODUCTION

Global environmental change has amplified biological exposure to a set of numerous ecological stressors, such as more ultraviolet (UV) radiation, atmospheric pollution and alterations in temperature (Lv et al., 2025; Pastorino et al., 2025). These stressors induce the oxidative process in various biological systems by causing an overproduction of reactive oxygen species (ROS), that affect cellular integrity and physiological functioning negatively (Fu et al., 2025; Jomova et al., 2023). Chronic oxidative stress has been linked with loss of the molecular

structure of biomolecules, inhibition of tissue regeneration, and decline in biological tolerance indicating the necessity for adaptive protective mechanisms in living systems (Fathi et al., 2025; Fekrirad et al., 2026).

Plants act as one of the first ecophysiological barriers in defense against environmental stress, because they are capable of synthesizing a number of secondary metabolites (Jangpangi et al., 2025; Linh & Duc, 2025). These chemicals including phenolics, flavonoids and triterpenoids are responsible for redox regulation, UV protection and stress tolerance (Shin & Lee, 2025; Suvedi et al., 2025). Secondary metabolite biosynthesis is not a static process, but represents an adaptive metabolic response to environmental stimuli such as light irradiation, temperature variation and oxidative stress (Aktar et al., 2025; Ryu et al., 2025). Therefore, natural metabolites from plants have become the focus of attention as sustainable functional materials for green research.

Centella asiatica plants are known to be rich in triterpenoid and phenolic compounds, especially asiaticoside, madecassoside, asiatic acid, and madecassic acid (Ali et al., 2025; Dewi et al., 2025). These metabolites possess potent antioxidant, anti-inflammatory and collagen modulating properties which aid in the protection of cells and repair of tissue (Fujii et al., 2008; Haftek et al., 2022; Jiang et al., 2025; Mukherjee et al., 2011; Sucharitakul et al., 2025). C. asiatica extracts have been shown to improve endogenous antioxidant systems and reduce oxidative damage caused by UV radiation and pollutants (Buraphaka et al., 2024; Hashim, 2011; Seevaratnam, 2012; Subathra et al., 2005).

In the last few years, green synthesis of metallic nanoparticles using plant secondary metabolites as biogenic reducing and capping agents has been developed. Green synthesis methods are a benign alternative to traditional chemical approaches, which can use toxic reagents and produce hazardous waste (Arulnangai et al., 2025; Das et al., 2017; Khatami & Iravani, 2021; Malik et al., 2023; Tripathy & Srivastav, 2023b, 2023a). During plant-assisted nanoparticle synthesis, phytochemicals have the roles of bioreducing metal ions and of stabilizing produce nanodomains, which is in concord with material production strategies following ecological sustainability principles.

Of these, gold nanoparticles (AuNPs) are especially appealing because of their inert nature, tunable surface plasmon resonance band (SPR), and biocompatibility. The optical properties of AuNPs are greatly influenced by their size, shape, and aggregation state and such aspects are responsible for both absorbing and scattering light (Linima et al., 2024; Noruzi, 2015; Pratap & Soni, 2021; Raszewska-Famielec & Flieger, 2022; Sobi et al., 2024; Soto et al., 2023; Wang et al., 2020). It has even been described that controlled aggregation of AuNPs increases the efficiency of UV scattering, indicating a nonlinear relationship between functional performance and colloidal stability (Ruth et al., 2024; Sharma et al., 2025; Thanayutsiri et al., 2020).

Synthetic polymers, such as polyvinyl alcohol (PVA), are among the most effective stabilizers in nanoparticle (NP) synthesis. This is due to their hydrophilic nature, their ability to induce steric stabilization, their incompatibility with acidic systems, and their high compatibility with aqueous systems (Manotham et al., 2023; Thanh et al., 2025). Their effectiveness in preventing aggregation and improving long-term colloidal stability has been well documented. However, there are green nanoparticle syntheses that use complex phytochemical matrices. These include Centella asiatica leaf extracts. The addition of PVA also causes complex phenomena. Polymers can compete with natural bioactive molecules to attach to the particle surface (competitive adsorption), disrupt initial nucleation kinetics, and alter the growth mechanism (Alguno et al., 2025; Khavani et al., 2024; G. Satpathy et al., 2020; S. Satpathy et al., 2020). Additionally, the possibility of bonding between PVA chains and natural polymer constituents of the extract may affect the final morphology, size distribution, and characteristics of the nanoparticles (Kumar et al., 2023). Consequently, PVA characteristics (e.g., concentration, molecular weight, and degree of hydrolysis) are important factors that must be considered and optimized in order to utilize its stabilizing effect while minimizing undesirable effects on the green process and functionality (Van Ngo et al., 2023; Zhang & Lee, 2024; Silva et al., 2024).

Much progress has been made in the green synthesis of AuNPs. However, how polymers help stabilize AuNPs and their impact on optical properties are not yet fully understood. This represents an important knowledge gap, as the functional performance of materials for example, in UV radiation treatment can be dominated by transient aggregation rather than long-term static colloidal stability. To address this, the current study employs an AuNPs synthesis protocol with Centella asiatica leaf extract and polyvinyl alcohol (PVA) as additional stabilizing agents. Through a detailed study of physicochemical and functional properties, we aim to determine the impact of polymer addition on nanoparticle growth kinetics, colloidal stability, aggregation dynamics, and UV response. The results will contribute to a more comprehensive design space for sustainable plant-based nanotechnology, balancing ecological compatibility and functionality without significantly compromising material integrity.

LITERATURE REVIEW

Plant Secondary Metabolites and Ecological Protection

Plants have developed adaptive defense mechanisms in response to various abiotic and biotic stresses (e.g., high-intensity UV exposure). These mechanisms are characterized by the synthesis of secondary metabolites (Lv et al., 2025; Pastorino et al., 2025). This process is known as adaptive defense signaling induced by environmental stress factors. These plant metabolites, such as phenolics, flavonoids, and triterpenoids, play a significant ecological role. This role includes redox homeostasis regulation, direct protection against UV light, and conferring cellular adaptability (Shin & Lee, 2025; Suvedi et al., 2025). They are dynamically synthesized, triggered by stress, and influenced by environmental factors such as light exposure and oxidative stress (Aktar et al., 2025; Ryu et al., 2025). Evolutionarily designed NCPs have become popular sustainable building blocks in green nanotechnology. In this field, they are used as reducing and stabilizing agents in the synthesis of metal nanoparticles used in biomedical applications (Arulnangai et al., 2025; Khatami & Iravani, 2021).

Centella asiatica as a Source of Bioactive Compounds

Centella asiatica is known to be rich in bioactive triterpenoid compounds such as asiaticoside, madecassoside, asiatic acid, and madecassic acid (Zhou et al., 2025). These metabolites have strong antioxidant, anti-inflammatory, and collagen modulating properties, which can contribute significantly to cell protection and tissue repair (L. Li et al., 2025; Mukherjee et al., 2011; Sucharitakul et al., 2025). Research shows that extracts of this plant can strengthen the body's natural antioxidant defenses and reduce oxidative damage caused by factors such as UV light (Buraphaka et al., 2024; Subathra et al., 2005). An additional contribution to this free radical scavenging and UV absorption capacity is provided by the presence of flavonoids and phenolic acids that work synergistically, indicating this source as an attractive provider of agents for plant protection (Haftek et al., 2022).

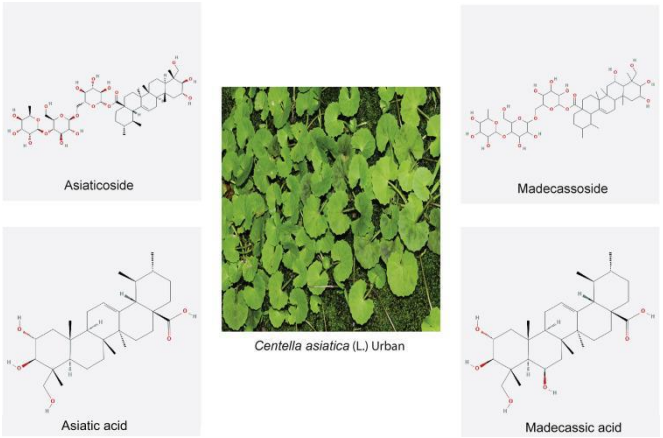

Figure 1. Bioactive compounds of C. asiatica.

Green Synthesis of Gold Nanoparticles Using Plant Extracts

Plant-mediated bio-reduction of gold salts and subsequent formation of AuNPs is eco-friendly compared to the chemical methods as conventional chemicals used in these synthesis often include toxic reagents (Das et al., 2017; Malik et al., 2023). Here, phytochemicals of plants such as Centella asiatica play a dual role, which is to the reduction process of gold ions (Au^{3+} to Au^{0}) and subsequently cover and stabilize the resulting nanoparticles against further aggregation (Khatami & Iravani, 2021; Noruzi, 2015). The detailed profile of the phytochemical matrix and reaction kinetics play a vital role in determining the physicochemical properties of the AuNPs such as its size, shape, stability (Linima et al., 2024; Sobi et al., 2024).

Polymer-Stabilized Gold Nanoparticles: Role of PVA

Synthetic polymers such as polyvinyl alcohol (PVA) are commonly employed and serve as secondary stabilizer for the synthesis of nanoparticles because they are hydrophilic, applying a steric barrier without allowing aggregation and contribute to a prolonged colloidal stability of the nanoparticle obtained (Manotham et al., 2023; Thanh et al., 2025). But in the green synthesis systems, with introduction of PVA there may have multiple interfacial kinetics. It can compete with natural phytochemicals for adsorption on nanoparticle surfaces (competitive adsorption), which may change nucleation kinetics and growth mechanisms (Khavani et al., 2024; G. Satpathy et al., 2020; S. Satpathy et al., 2020). This interaction has a bearing on final particle size distribution and

polydispersity, meaning the addition of polymer must be tuned to strike a balance between increased stability with maintaining the original green synthesis pathway (Nakra et al., 2025; Rakshit et al., 2025).

UV Radiation, Oxidative Stress, and Functional UV Protection

UV radation is an environmental stressor causing oxidative stress, producing reactive oxygen species (ROS), which in turn cause degradation of various biologically important molecules and promote aging (Fu et al., 2025; Jomova et al., 2023). Efficient protection against UV radiation involves not only the chemical absorption, but also the physical scatter of incident rays. Of most interest in this regard are AuNPs because their surface plasmon resonance can be adjusted and thus they strongly couple to light. Their performance with respect to UV protection is also a function of their aggregation, and controlled aggregation can lead to enhanced light scattering that may result in optimizing them for function rather than maximizing colloidal dispersion (Pratap & Soni, 2021; Raszewska-Famielec & Flieger, 2022).

Conceptual Framework of the Study

The basis of this work is a conceptual model that connects plant bioactive compounds, green-synthesized AuNPs, polymer stabilization and UV protection functionality. The centella asiatica extract is a reducing and capping agent, controlling both the formation of nanoparticles as well as the surface chemistry. The presence of PVA changes the dynamics of particle growth and colloidal stability, which determines optical properties and UV protection performance. This model focuses on the compromise between long-term stability and functioning performance, thus making explicit the non-linear correlation between synthesis conditions and application performance.

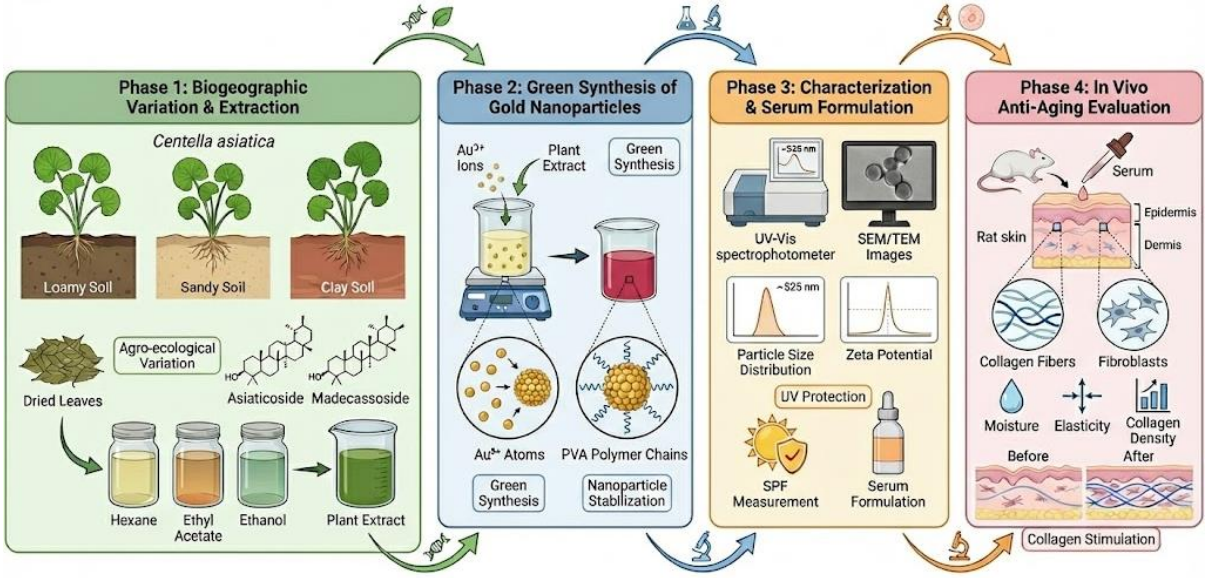

Figure 2. Research Scheme for Centella asiatica Gold Nanoparticles for Anti-Aging

METHOD

Preparation of plant extract

Fresh leaves of Centella asiatica were employed as raw material for the preparation of bioactive extract which could be served as reducing and capping agent. The plant material was rinsed, air dried and oven-dried at room temperature until a constant weight was obtained. The dried mass was milled followed by sieving using mesh 120 to give a fine powder. Extract preparation followed a maceration procedure to maintain the activity of thermolabile secondary metabolites, and an organic solvent fixative. The mixture was alternately agitated and filtered, and the extraction procedure was repeated for maximization of metabolite yield. The combined filtrates were concentrated in vacuo on a rotary evaporator at reduced temperature to give the final product without the solvent. The final crude extract was kept in air-tight vessels while avoiding light until it was used for the nanoparticle preparation. This extraction methodology is standard to retain phytocompounds integrity, mainly in green synthesis system (Aktar et al., 2025; Das et al., 2017; Nakra et al., 2025).

Green Synthesis of Gold Nanoparticles

Green reduction method was employed to synthesize gold nanoparticles by treating aqueous chloroauric acid ($HAuCl_4$) solution with C. asiatica extract. The method involved dropwise addition of the extract to the gold precursor with vigorous stirring and careful heating. The reaction was observed both by the colour change and spectrophotometrically for nanoparticle formation. The effect of polymer stabilization was also studied; poly (*vinyl alcohol*) (PVA) solutions in known concentrations were added as a second stabilizer to the selected formulations. Two preparation methods were included: AuNPs without PVA (−PVA) and AuNPs with matching addition of PVA (+PVA). The reaction temperature and time were optimized to induce nucleation and, at the same time, prohibit a disorderly aggregation. The reaction was obtained from previously published green nanoparticle synthesis techniques (Anandan et al., 2025; Rakshit et al., 2025).

Physicochemical Characterization of Nanoparticles

The AuNPs prepared were analyzed in various ways. Surface plasmon resonance bands were observed by UV–Vis spectroscopy and colloidal stability was monitored as a function of time. Dynamic light scattering-based particle size distribution and polydispersity index analyses were performed with the aid of a particle-size analyzer (Ruth et al., 2024; Soto et al., 2023). Zeta potential and conductivity were measured to determine surface charge and colloidal stability, respectively. SEM was used to investigate morphological aspects and particle agglomeration. Chemical interaction among phytochemicals, PVA and gold surfaces were investigated by the FTIR and the elemental composition was identified by EDX. These methods combined give a full insight into the structure, stability and surface properties of nanoparticles (Raszewska-Famielec & Flieger, 2022) .

Evaluation of UV-Protective Performance

The UV protective ability of the prepared AuNPs was assessed using the Sun Protection Factor (SPF) based measurements and characterized by UV–Vis spectrophotometry. Nanoparticle solutions were further diluted to predetermined concentrations for UV scanning in the UV region applicable to UV-B light. SPF values were calculated by a mathematical approach based on measured absorbance at constant wavelength intervals. Measurements were taken at several time points for the evaluation of temporary evolution and protection. This technique allows testing of functional behaviour with respect to nanoparticle aggregation and stability kinetics (Moumita, 2017; Rezky Putri et al., 2020).

Table 1. Analytical techniques and key parameters used for characterization and UV-protective evaluation of gold nanoparticles

Analysis	Instrument/Method	Key Parameter
Optical properties	UV–Vis spectrophotometry	SPR wavelength
Particle size	PSA (DLS)	Z-average, Pd index
Surface charge	Zeta potential	Stability indicator
Morphology	SEM	Shape and aggregation
Chemical interaction	FTIR	Functional groups
Elemental composition	EDX	Au confirmation
UV protection	UV–Vis SPF analysis	SPF value

Statistical Analysis

All tests were carried out in triplicate and results are shown as mean ± SD. The differences were analyzed statistically using a one-way analysis of variance comparing nanoparticle formulations with and without PVA. Normality and homogeneity of the data were tested before comparisons. Between-group differences were tested with suitable parametric tests, with post hoc comparisons used upon identifying significant differences. Evidence was considered significant at $p < 0.05$ for all statistical analyses. This methodology secures a solid interpretation of the physico chemical and functional differences among formulations (Ghozali, 2011).

RESULTS

Visual Formation and Optical Confirmation of Gold Nanoparticles

The formation of the gold nanoparticles (AuNPs) obtained with the Centella asiatica extract was first visually confirmed by a color change in solution consisting of AuNPs and uncapped reacted extract. The color of the solution transformed from pale yellow to ruby red and purple that usually referred to reduction of Au^{3+} ions to

Au^0 nanoparticles. Color developed at rate and temperature dependent on formulation, suggesting differences in reaction kinetics. Colour was formed initially much faster in systems devoid of poly (vinyl alcohol) (PVA), indicating that nucleation and particle growth were faster. On the other hand, PVA formulations also showed gradual changing of color, but had persistent being intensity over a long time.

UV–Vis spectrophotometer study of the synthesized AuNPs also verified the formation of AuNP based on the development of well-defined surface plasmon resonance (SPR) absorption peaks. All the formulations showed SPR peaks at 535–547 nm which is typical of spherical gold nanoparticles. The similar λmax values of all formulations suggest that the core particle structure was quite conserved, even under different stabilizing environments. Together, this set of optical measurements reveals successful nanoparticle formation and early evidence that the involvement of PVA is in reaction kinetics (and not responsible for the general formation process of nanoparticles).

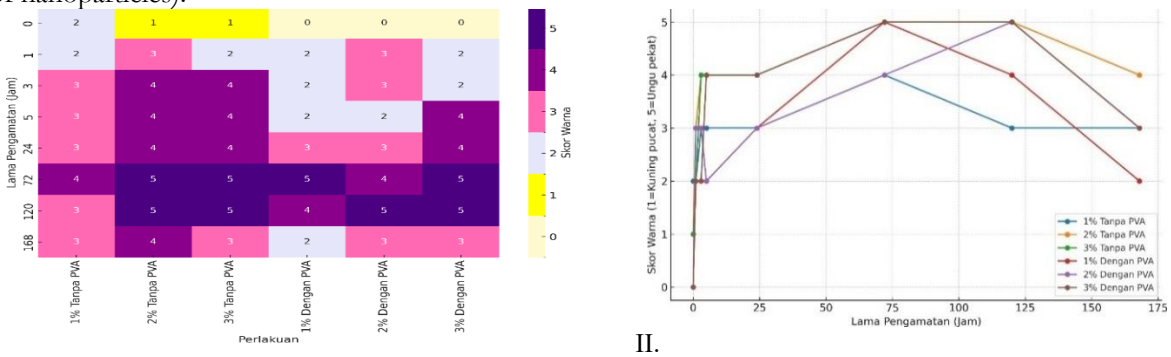

Figure 3. Visual color evolution and UV–Vis SPR confirmation of AuNP formation with and without PVA.

Effect of PVA on Optical Stability and Absorbance Behavior

From Table 2, it is clear that there are obvious distinctions regarding the optical response and temporal stability between AuNPs prepared with PVA reduction and those without. The λ_max in all formulations across the reactivity time was quite similar (539 to 547 nm), suggesting that the important plasmonic features as well as particle size distribution of the AuNPs remained mostly unchanged throughout the monitoring. The observed stability of λ_max also implies that no substantial chemical transformation or noticeable morphological degradation took place with storage time.

But significant differences were seen in absorbances indicating that there are differences in colloidal stability. AuNPs without PVA exhibited high values of absorbance during the initial storage time (24 to 72 h) and a subsequent decrease at longer periods (120 to 168 h). This tendency was a most representative in the 3% extract as absorbance reached its maximum at approximately 0.648 after which it decreased with time to be up to 0.532. This implies a deaggregation or partial precipitation process over time, leading to the decrease in effective optical density.

On the contrary, AuNPs prepared using PVA resulted in a more restrained evolution of the absorbance. While the initial (peak-absorbance) absorbance of most samples was reduced compared to PVA-free systems, decrease during prolonged storage was less evident. For instance, in the 2% extract with PVA formulation absorbances values kept more or less constant over time (ranged up and down around a certain value) but were also higher even at 168 hours than those for the corresponding PVA-free samples. This indicates that PVA is efficiently steric stabilizer thereby preventing the aggregation of NPs and improving the long-term optical stability.

As can be seen from Table 1, the PVA has no noticeable effect on plasmon resonance position of AuNPs, but is very important in governing the absorbance stability with time. The presence of PVA confers the colloidal stability during storage, which makes it an efficient stabilizing agent in green-synthesized AuNP systems.

Table 2. λmax and absorbance evolution of AuNPs synthesized with and without PVA over time.

Sample	ntrasi	λmax	absorbansi	λmax	absorban si	λnax	Absorbansi	λmax	absorban si	λmax	absorban si	λmax	absorban si
Nano partikel	1 %	543	0,434	544	0,44	541	0,364	539	0,51	545	0,28	545	0,91
Emas	2 %	544	0,554	544	0,55	544	0,364	538	0,44	544	0,50	545	0,95

Sampl e	nt ra si	λ m a x	abs or ban si	λ m a x	abs o rba n si	λ m a x	Abs orba nsi	λ m a x	abs o rba n si	λ m a x	abs o rba n si	λ m a x	abs o rba n si
Ekstra k		2	0,443	2	7	1	4	1	8	4	4	2	4
Pegag a n + PVA	3 %	5 4 6	0,540	5 4 4	0,4 4 1	5 4 5	0,423	5 4 6	0,4 1 9	5 4 6	0,4 0 3	5 4 3	0,3 7 2
Nano pa rtikel	1 %	5 4 1	0,723	5 4 1	0,5 4 9	5 4 1	0,58 2	5 3 6	0,6 1 7	5 3 8	0,7 6 9	5 4 1	0,3 7 3
Emas	2 %	5 4		5 4	0,7 2	5 4	0,67	5 4	0,4 3	5 4	0,7 0	5 4	0,5 7
Ekstra k		3	0,648	3	0	3	8	3	4	4	2	4	1
Pegag a													
n Tanpa	3 %	5 4 7		5 4 6	0,6 4 8	5 4 7	0,633	5 4 4	0,5 6 8	5 4 2	0,6 3 3	5 4 0	0,5 3 2
PVA													

Particle Size Distribution and Polydispersity

Fig. 4 The size distributions of the AuNPs synthesized with and without poly(vinyl alcohol) (PVA). Without the PVA, the narrow characteristic peak of size distribution curve slightly shifts to sub-100 nm, indicating that a dominant particle component with a moderate degree of agglomeration is present. The appearance of a minor (small) secondary peak at higher diameters indicates little pre-association and formation of large aggregates is not substantial to overall intensity. This distribution is consistent with a structure stabilized mainly by the phytochemical capping agents present in Centella asiatica, which affords sufficient surface coverage to restrict uncontrolled overgrowth of particles but still allows some degree of coalescence.

On the other hand, AuNPs prepared in the presence of PVA present a broader and higher intensity distribution main maximum at much larger hydrodynamic diameters. Extended distribution and tail to larger size range suggest enhanced polydispersity and the existence of large hydrodynamic agents. This behavior implies that PVA changes dispersion environment which causes the formation of weakly bound nanoparticle clusters or polymer-bridged aggregates those appear as larger particles in DLS results. However, for a system of just one such large peak, it will still only appear as having grown in size but is not a permutation with (*processive*) aggregation behaviour. In general, PSA data have proven that the presence of PVA induces a significant change in the hydrodynamic size distribution of AuNPs, increasing both its size and those ones related to LAct-2 and LAct ∼σ compared to pure AuNPAs-free systems.

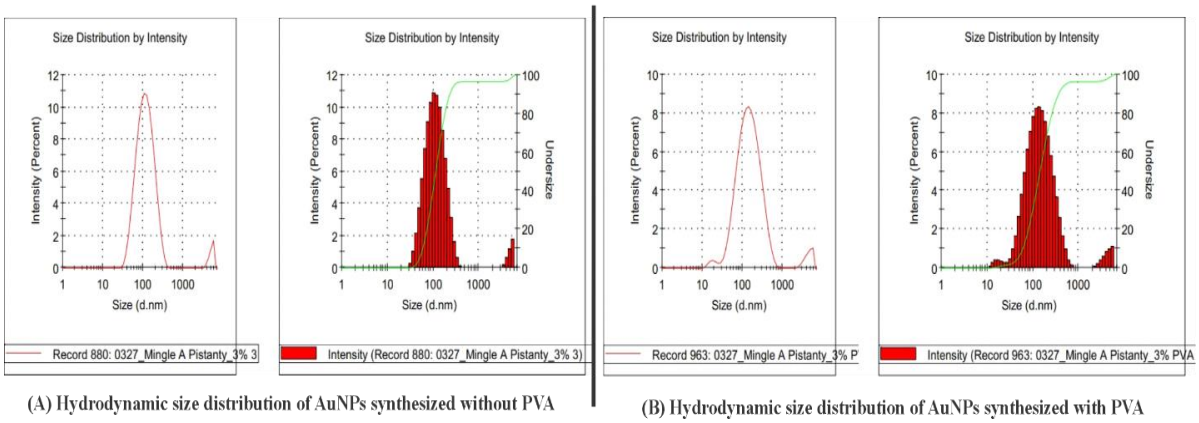

(A) Hydrodynamic size distribution of AuNPs synthesized without PVA

(B) Hydrodynamic size distribution of AuNPs synthesized with PVA

Figure 4. Hydrodynamic size distribution of AuNPs synthesized with varying extract concentrations, with and without PVA.

Table 3. summarizes the particle size analysis and shows that both the plant extract concentration and poly(vinyl alcohol) (PVA) play an important role in controlling the hydrodynamic size distribution and dispersity of the generated AuNPs. AuNPs prepared in absence of PVA experienced the more apparent concentration-induced size increase. The Z-average size doubled from about 74.60 nm at 1% extract concentration to 99.02 nm at 3%, signifying a progressive increase in the particle size with increasing availability of phytochemical reducing and capping agents. This tendency was also well observed in the D50 and D90 values of 1% and 3%, respectively, approximately increasing from ca., 89.93 nm & 241.00 nm to ca.,114.33 nm &237.33nm, indicating that larger hydrodynamic species were formed as a function of increased extract concentrations.

The polydispersity index (PdI) of PVA-free AuNPs was 0.396 at 1%, 0.352 at 2% and 3%, showing low-medium polydispersity with a slight improvement in size uniformity by further increasing the extract concentration. Peak 1 also obviously increased in size, from 68.75 nm (at 1%) to 124.67 nm (at 3%), while the respective peak intensities remained high (>87%), indicating the presence of a major population Bandow et al., maintained for all particle sizes instead of constituting newly added largest particles.

On the other hand, the impregnation of PVA led to a significant enhancement in particle size regardless of extract concentration. The Z-average diameters were significantly increased at 1%+PVA (115.83 nm) and peaked at 2%+PVA (143.50 nm), then slightly reduced to 121.00 nm at 3%+PVA. This non-monotonic behavior reveals that PVA changes the growth and aggregation trend of AuNPs. The corresponding D90 values were significantly increased in PVA containing systems, which could reach 459.00 nm at 2%+PVA (indicating larger aggregation or member clusters).

PdI values were higher in PVA-stabilized samples than thosewithout PVA, especially for 2%+PVA (PdI ≈ 0.420), denoting an enhanced polydispersity. Peak 1 sizes with PVA were consistently larger, varying from ~152.40 to 199.70 nm and peak intensities for all samples>90%, signifying the increased hydrodynamic diameters associated a predominant particle population rather than outliners of sporadic particles. In general, these findings show that as the extract concentration increases, AuNPs growth in absence of PVA is favored, and its presence results in higher polydispersity values and larger hydrodynamic sizes, evidencing a high influence on nanoparticle dispersion features.

Table 3. Summary of PSA-derived size parameters (Z-average, PdI, D10–D90).

Concentration of Centella asiatica extract	**Z-Avg (nm) (Mean ± SD)**	**Pd Index (Mean ± SD)**	**Peak 1 Size (d.nm) (Mean ±**	**Peak 1 Int (Mean ± SD)**	**D10 (nm) (Mean ± SD)**	**D50 (nm) (Mean ± SD)**	**D90 (nm) (Mean ± SD)**
(L). Urb			**SD)**				
1%	74.60	0.396	68.75	87.70	37.83	89.93 ±	241.00
	1.50	0.007	57.07	1.05	2.30	1.03	± 1.73
2%	89 ± 0.44	0.352	116.00	91.40	54.03	104.67 ±	194.00
		0.004	0.69	0.36	1.25	0.58	± 8.49
3%	99.02	0.352	124.67	96.10	59.87	114.33 ±	237.33
	3.23	0.007	0.76	1.28	0.71	0.58	± 13.57
1%+PVA	115.83	0.385	152.40	92.10	59.60	133.67 ±	303.67
	2.30	0.011	5.37	0.55	1.30	3.79	± 11.85
2%+PVA	143.50	0.420	199.70	93.67	67.57	168.67 ±	459.00
	3.12	0.011	3.01	1.51	3.44	4.51	± 43.60
3%+PVA	121.00	0.378	164.37	92.73	62.07	141.67 ±	352.67

Concentration of Centella asiatica extract	Z-Avg (nm) (Mean ± SD)	Pd Index (Mean ± SD)	Peak 1 Size (d.nm) (Mean ±	Peak 1 Int (Mean ± SD)	D10 (nm) (Mean ± SD)	D50 (nm) (Mean ± SD)	D90 (nm) (Mean ± SD)
	1.97	0.005	4.25	2.47	1.63	2.31	± 38.65

Zeta Potential and Colloidal Stability

Figure 5 displays the zeta potential distribution patterns of gold nanoparticles (AuNPs) prepared with Centella asiatica extract at various concentrations in the absence (A1–A3) and presence of polyvinyl alcohol (PVA, B1–B3). All formulations in the PVA-free series (A1–A3) showed mainly negative zeta potential peaks, which were attributed to negatively charged surface groups originating from plant phytochemicals. An apparent trend was identified that as extract concentration increased, the zeta potential peak shifted to less negative values, implying diminishing electrostatic repulsion and the more pronounced aggregative tendency at higher concentrations.

On the other hand, AuNPs prepared with PVA (B^1–B^3) exhibited more well-defined and symmetrical zeta potential distributions and peak positions consistently located in the strongly negative area. The more narrow peak widths and greater peak intensities of the PVA-containing samples suggest a homouniform surface charge distribution and superior colloidal homogeneity. The fact that strongly negative zeta potential values are maintained exposing improved colloidal stability, due to a combination of electrostatic stabilization contributed by plant based anionic groups and steric stabilization exerted by the adsorbed PVA chains. On the whole, zeta potential profiles reveal that although in the presence of phytochemicals alone AuNPs provide with a base electrostatic stability; upon incorporation with PVA an optimized charge-distribution is provided which complement AuNP- dispersions to achieve long term colloidal stability.

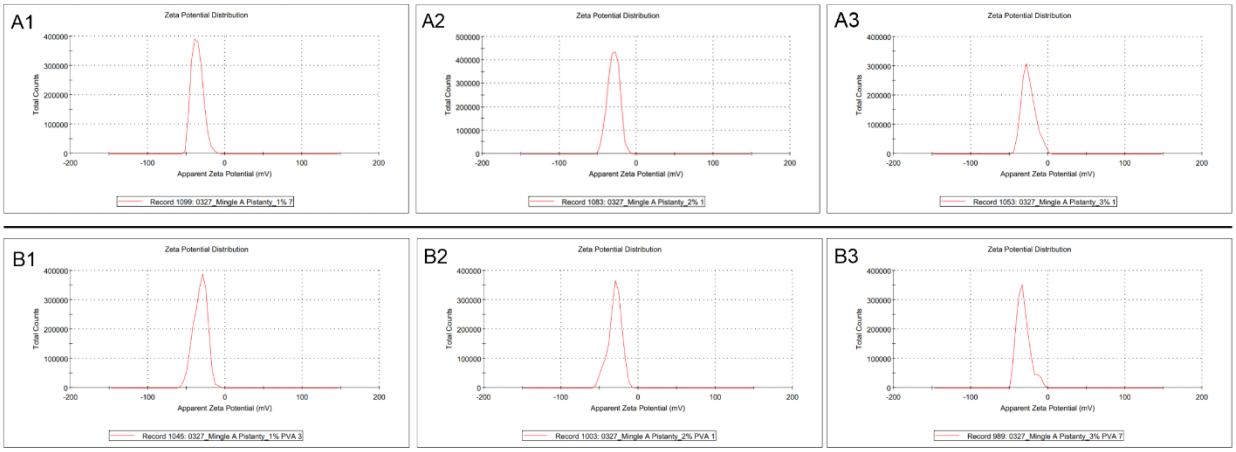

Figure 5. Zeta potential profiles of AuNPs synthesized with and without PVA.

Measurements of zeta potential and conductivity show different colloidal behavior in AuNPs prepared with or without PVA. In systems without PVA, an increase in extract concentration from 1% to 3% causes a progressive shift in the average zeta potential toward less negative values, from −34.60 mV to −25.80 mV. This trend indicates a decrease in electrostatic repulsion between nanoparticles as the extract concentration increases, which typically causes high aggregation due to this effect. Meanwhile, conductivity increases with extract concentration, indicating a higher free ion content in the dispersion medium, which may be due to free phytochemical components. Meanwhile, the zeta potential of AuNPs produced from PVA remained negative (+PVA) at all concentrations and was even more negative (−30.33 mV) for the 3%+PVA system compared to the system without PVA. In the case of cells cultured in a medium containing PVA, lower TC values were obtained, especially in the 3+PVA system, indicating a decrease in ion mobility in the medium. A higher negative zeta potential with low conductivity describes improved colloidal stability due to the addition of PVA. In general, the data show that electrostatic stabilization by phytochemicals is dominant in systems without PVA, and the presence of PVA alters the surface charge and ionic composition, which affects the long-term stability of the dispersion.

Table 4. Zeta potential and conductivity values of AuNP formulations.

Group Sample	**Average Zeta Potential (mV) ± SD**	**Average Conductivity(mS/cm)**
1%	-34,60 ± 1,06	0,0625 ± 0,0002
2%	-29,97 ± 1,48	0,0651 ± 0,0008
3%	-25,80 ± 0,76	0,0677 ± 0,0011
1%+PVA	-32,50 ± 0,89	0,0485 ± 0,0004
2%+PVA	-29,80 ± 1,50	0,0499 ± 0,0012
3%+PVA	-30,33 ± 1,44	0,0157 ± 0,0002

Morphological Characteristics by SEM

SEM images of GNPs produced from Centella asiatica extracts at different concentrations (1%, 2%, and 3%) without PVA addition (A) and with PVA addition (B) are shown in Figure 6. Without PVA (A1–A3), AuNPs mostly had spherical and sub-spherical shapes with severe particle-particle contact, which settled into dense and compact aggregates. The intensity of aggregation increased with the concentration of the extract; from sparser particles at 1% (A1) to large and irregular clusters at 2% and 3% (A2–A3). These small particles indicate weak steric hindrance and are dominated by phytochemical-mediated electrostatic interactions. The aggregation behavior of samples containing PVA (B1–B3) was markedly different from that of other samples. Although there was still evidence of particle aggregation, the aggregate structure was more open and less compact, with larger spaces occupied by individual particles. The addition of PVA resulted in a more uniform distribution of AuNPs on the substrate, especially at higher extract concentrations, indicating that interparticle interactions had been modified. However, although the size appeared to increase due to PVA modification in some cases, the aggregates had a looser structure, supporting that the function of PVA was to modify the architecture rather than prevent sintering. Overall, the SEM study validates that the aggregation density is influenced by the extract concentration and that the addition of PVA changes the shape and arrangement pattern of the AuNPs aggregates.

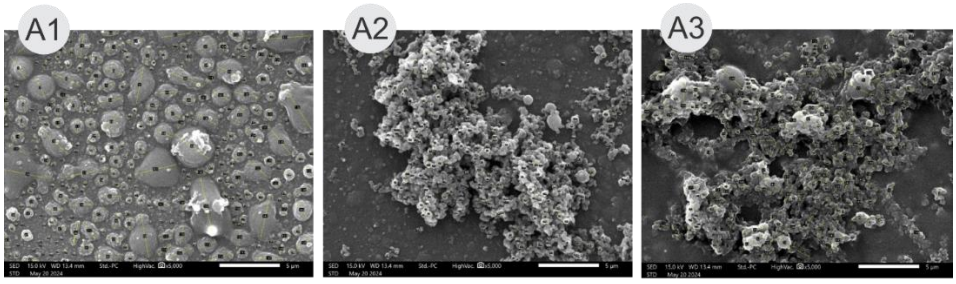

SEM Image Results of 1% (A1), 2% (A2), and 3% (A3) Gotu Kola Extract Without PVA Addition

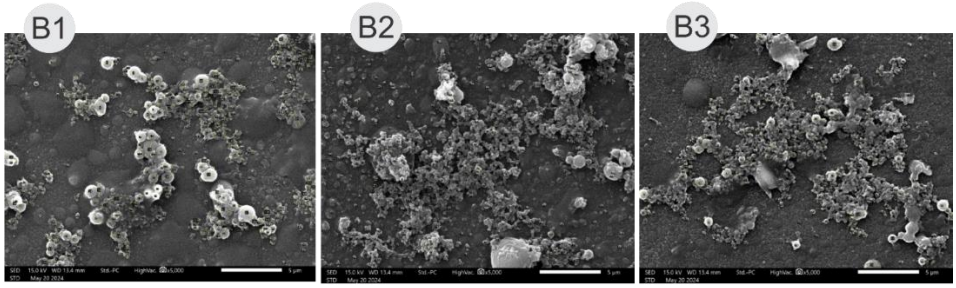

SEM Image Results of 1% (A), 2% (B), and 3% (C) Gotu Kola Extract with PVA Addition

Figure 6. SEM micrographs of AuNPs synthesized with and without PVA.

Functional Evaluation: Sun Protection Factor (SPF)

The SPF value of gold nanoparticles (AuNPs) synthesized from Centella asiatica extract varies depending on the concentration of the extract, polyvinyl alcohol (PVA), and storage time (Table 5). The SPF value of AuNPs samples made without PVA was always higher than those using PVA for all observation times. At the first observation, higher extract concentrations caused a progressive increase in SPF values in both systems, but without PVA as a stabilizer, this was much more pronounced; at the same substance load ≥10%, both concentrations provided significantly higher UV protection (20-30%) compared to samples containing PVA. A clear temporal dimension was observed on the third day of storage, with increasing SPF values for AuNPs without PVA, especially at higher extract concentrations, which reached approximately one order of magnitude higher than the highest values measured during the study. On the other hand, the formula containing PVA showed a decrease in SPF

values at the same time interval, especially at lower extract concentrations. After a longer storage period (days 5 and 7), the SPF values recorded in both systems showed lower variation, but were always higher for AuNPs without PVA. Overall, these results indicate the beneficial effect of extract concentration on SPF and a clear trade-off between sun protection effectiveness and stability when PVA is added to improve colloidal stability.

Table 5. Comparative SPF values across formulations and storage time.

Storage time (day)	AuNPs + PVA (1%)	AuNPs + PVA (2%)	AuNPs + PVA (3%)	AuNPs – PVA (1%)	AuNPs – PVA (2%)	AuNPs – PVA (3%)
1	0.55	2.84	4.24	1.00	4.46	6.39
3	0.53	1.93	3.81	4.84	8.82	9.66
5	1.34	3.54	4.95	2.6	5.27	8.76
7	3.58	5.88	6.07	2.42	5.73	8.93

Spectroscopic Evidence of Capping Interactions (FTIR)

Figure 7 shows the FTIR spectra of Centella asiatica extract and corresponding AuNPs in the presence/absence of polyvinyl alcohol (PVA) for different extract concentrations. In all spectra, we observed broad absorption bands in the 3200–3500 cm^{-1} region, which are attributed to O–H stretching vibrations characteristic of hydroxyl groups commonly found in phenolic compounds, flavonoids, and triterpenoids present in plant extracts. Intense bands in the 2920–2850 cm^{-1} region and around 1600–1650 cm^{-1} are attributed to aliphatic C–H stretching and C=O (and/or aromatic C=C) stretching, respectively. In the synthesis of AuNPs without PVA (A1–A3), bands associated with O–H and C=O groups bound to it caused shifts and changes in intensity corresponding to those found in the extract spectrum, reflecting that these groups participated in nanoparticle reduction and surface coating. For formulations B1, B2, and B3 containing PVA, new spectral bands were observed at PVA-specific vibrations, particularly C–O stretching and C–H deformation vibrations. The appearance of extract-related functional groups alongside PVA bands provides evidence of phytochemicals and polymers on the nanoparticle surface. Overall, the FTIR results provide clear spectroscopic evidence that the AuNP surface is coated with plant-based biomolecules and show that the addition of PVA affects the surface chemistry through co-adsorption rather than completely removing the phytochemical coating.

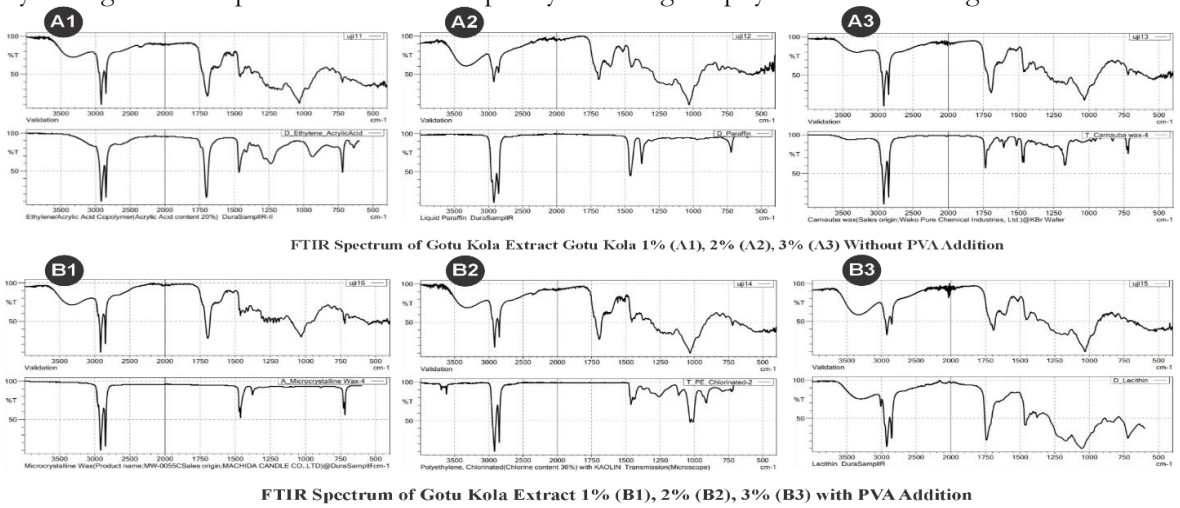

Figure 7. FTIR spectra of plant extract, AuNPs, and AuNPs–PVA formulations.

The FTIR spectrum in Figure 6 and the target peaks (Table 6) show that changes in transmission intensity (%T) occur systematically in each plant extract, AuNPs, and AuNPs–PVA system, which is related to surface chemical variations during nanoparticle formation. In plant extracts, the broad O–H stretching band (3300–3500 cm^{-1}) shows lower absorption compared to other peaks above it, indicating the highest absorption due to the high hydroxyl-containing phytochemical content. This band was observed to increase in %T after nanoparticle synthesis accompanied by a minor low shift, suggesting that a small number of OH groups may have been utilized during the reduction and capping process. For samples containing PVA, the O–H feature at around 3300 cm^{-1} became slightly narrower but with a decrease in %T compared to AuNPs samples without PVA, indicating partial overlap of absorption from PVA hydroxyl groups.

All the samples showed medium absorption in the aliphatic C–H stretching region (2900–2800 cm^{-1}). In comparison to the plant extract formation of AuNP caused a slighter increase in %T (ie lower absorption),

however, in the case of PVA containing formulations even lower absorbances were observed which was owed to further contributions from the polymer. The %T of AuNPs revealed a clear enhancement of the carbonyl-related (1600–1650 cm^{-1}) with a change in peak position to lower wavenumbers, attributing carbonyl or aromatic groups forming coordination bond onto the surface of gold. In AuNPs–PVA, a sharp band at 1700–1730 cm^{-1} with loss of intensity %T was also observed indicating residual acetate groups present in PVA. Mean %T of these bands also had average reductions after nanoparticle synthesis: strong C–O stretching bands between 1000 and 1200 cm^{-1} is a good example that showed relatively mild increases in %T =*f* (S/N) while PVA samples displayed decreased %T as a result of polymer absorption overlapped. In general, percentage FTIR profiles revealed the reduction of phytochemical absorption after the synthesis of AuNPs and emergence of further polymer absorption in PVA-protected system, proving co-capping interactions at NP surface.

Table 6. Assignment of key FTIR bands and functional group interactions.

Wavenumber (cm^{-1})	**Functional group**	**Sample**	**Observation**
3300–3500	O–H stretching (phenols, alcohols)	Plant extract	Broad and intense band
-3300	O–H stretching (PVA hydroxyl)	AuNPs–PVA	Slight shift to lower wavenumber vs. pure PVA
2900–2800	C–H stretching (aliphatic)	All samples	Present with reduced intensity in AuNPs
1600–1650	C=O / C=C stretching	Extract, AuNPs	Shift and intensity change after AuNP formation
1700–1730	C=O stretching (residual acetate, PVA)	AuNPs–PVA	Clearly observed
1000–1200	C–O stretching	Extract, AuNPs	Strong band, minor variation
-1060–1080	C–O stretching (PVA)	AuNPs–PVA	Strong and distinct
-840–850	C–C stretching (PVA backbone)	AuNPs–PVA	Weak but detectable

Note: AuNPs = gold nanoparticles; PVA = poly *(vinyl alcohol).*

Elemental Composition of AuNPs

EDX analysis was used to determine the elemental composition of the gold nanoparticles (AuNPs) obtained. As shown in Table 7, there was a clear difference in surface composition between formulations containing PVA and those without PVA. In AuNPs prepared with 1% extract without PVA, carbon (C) and oxygen (O) were the main elements present, with C found in the range of approximately 41.23–57.11% by weight and O contributing 36.41–38.10% by weight of the survey location. The high percentages of carbon and oxygen also indicate good surface coverage by organic substances produced from phytochemical coatings synthesized from Centella asiatica. The element that appeared in the range of 6.48–20.67% by weight was silicon (Si), which originated from the substrate or sample holder, which is often seen in SEM–EDX analysis.

When PVA was added to AuNPs synthesized using a 1% extract, carbon remained the main element, with a weight percentage of between 40.58 and 43.85%, and oxygen contributed around 4.08 to 41.11% by weight. The presence of nitrogen (N) at low levels (approximately 1.11% by weight) in one of the areas studied indicates the presence of nitrogen-containing organic residues, possibly related to minor phytochemical components or contaminants associated with polymers. The relative increase in carbon and shift in the C/O ratio in PVA-coated samples compared to those without PVA indicates the presence of additional organic material on the NP surface, consistent with polymer adsorption.

For AuNPs prepared using 2% extract without PVA, lower carbon content (up to 5.00% by weight) was observed in several other regions, along with detectable amounts of oxygen and silicon. Changes in atomic percentage, particularly the increase in the proportion of nitrogen in one region, indicate surface heterogeneity and local accumulation of organic residues. In contrast, AuNPs prepared using 2% extract and PVA had significantly higher carbon and oxygen contents, with a maximum of 88.27% for carbon and up to 46.02% for oxygen. These high values indicate a thicker organic layer, resulting from an integrated surface coating of phytochemicals and polymers. In general, based on EDX analysis, AuNPs are coated with organic content (C and O), consistent with complete coating by plant-derived components, plus the addition of PVA further leads to a more organic surface, supported by input from the co-coating process from FTIR and SEM images.

EDX results showed a sharp increase in surface oxygen and carbon content at a 3% extract concentration compared to lower concentrations. This explains the increased density of AuNP surface coverage by organic moieties derived from phytochemicals. In the case of 3% without PVA, oxygen and carbon became the dominant elements in both weight percentage and atomic fraction. This configuration was also consistent with the increase in Centella asiatica phytochemicals. These were the main layer at higher extract concentrations. The presence of nitrogen (N) in Area 2 indicates the involvement of nitrogen-containing biomolecular compounds, reflecting increased surface heterogeneity at higher extract concentrations. Conversely, the 3% + PVA sample shows a significant contribution due to the stronger influence of polymers and substrate contributions, as well as evidence of several organic components. The presence of C and O in both systems indicates that phytochemical coatings are present, even when concentrations are increased even further. The addition of PVA further alters the surface composition. The same applies to particle size, stability, and functional SPF performance, as suggested by differences in composition. The relationship between extract concentration and polymer stabilization is non-linear.

Table 7. Elemental composition of AuNPs determined by EDX analysis.

Sample	Area	Element	Weight (%)	Atomic (%)
1%	1	C	57.11	62.8
		O	36.41	30.79
		Si	6.48	3.64
	2	C	41.23	41.46
		O	38.1	37.9
		Si	20.67	20.62
1% + PVA	1	C	43.85	62.8
		O	41.11	30.79
		Si	50.38	3.07
	2	C	40.58	94.03
		N	1.11	1.44
		O	4.08	4.64
		Si	57.22	37.03
2%	1	C	27.59	40.81
		O	6.13	0.3
		Si	1.34	1.02
		N	1.11	60.8
	2	C	5	24.87
		O	11.29	0.3
		Si	6.64	1.13
2% + PVA	1	C	88.27	61.07
		O	33.12	43.72
		Si	18.21	15.44
	2	C	45.23	50.39
		O	46.02	57.44
		Si	8.74	8.23
3%	1	C	22.44	27.4
		O	29.41	40.3
	2	C	41.1	41.05
		O	41.72	41.04
		Si	4.41	2.68
		N	28.35	3.32
3% + PVA	1	C	44.55	51.8
		O	18	40.21
		Si	88.34	40.47
	2	C	21.54	37.78
		N	24.34	5.7
		O	24.74	30.7
		Si	18	4.02

DISCUSSION

In this study, it was revealed that the green synthesis of gold nanoparticles (AuNPs) using Centella asiatica leaf extract is not merely an interaction between multicellular organisms and nanoparticles. It is also a complex network of nonlinear phytochemical characteristics and event relationships. This underlies the direct relationship between synthesis conditions, physicochemical properties, and performance. The role of phytochemicals in gold ion reduction and nanoparticle closure was proven through comprehensive characterization (UV-Vis, PSA, zeta potential, SEM, FTIR, and EDX). This is in line with the principles of green synthesis from plants (Das et al., 2017; Khatami & Iravani, 2021).

An important finding is the dual nature of PVA, which has many applications in various fields. Its presence in complex phytochemical systems causes an increase in hydrodynamic diameter and polydispersity, despite its known role in contributing to colloidal stability through steric hindrance (Manotham et al., 2023; Thanh et al., 2025). This suggests that, in green synthesis media, PVA plays an active role in competing with native bioactive components (e.g., triterpenoids and phenolics) released from C. asiatica for active binding sites on the AuNP surface (Khavani et al., 2024; G. Satpathy et al., 2020; S. Satpathy et al., 2020). This combination of competition and the particles' ability to engage in polymer bridging may result in incomplete surface coverage by phytochemicals. This can lead to loose aggregates with an apparent increase in particle size, without macroscopic precipitation a common observation in other bio-nano complex interfaces.

The colloidal properties, indicated by zeta potential and conductivity analysis, are both evidence to reveal that all the synthesized AuNPs possess negative charges which may come from deprotonated phenolic and carboxylic groups of the plant metabolites (Shin & Lee, 2025; Suvedi et al., 2025). The presence of PVA, in particular at higher concentrations, increased the long term stability indicated by constant zeta potential value and decreased conductivity. This suggests that the stabilization mechanism is mainly due to the steric interaction by the polymer rather than electrostatic repulsion effects (Fan et al., 2025). Importantly, this enhanced colloidal stability did not correspond directly to improved functional performance thus demonstrating a key discrepancy between physical-chemical stability and application-specific effectiveness.

These findings are further supported by spectroscopic analysis and elemental studies. FTIR spectra also confirm the presence of functional groups (O–H, C=O) from plant secondary metabolites in the reduction and closure of nanoparticles. These characteristic bands are still observed in PVA samples, indicating tandem polymer and phytochemical coating rather than replacement by polymers (C. Li et al., 2025; Thanh et al., 2025). EDX showed high carbon and oxygen content, which is associated with organic surface layers, with a more prominent maximum in the case of PVA addition (Manotham et al., 2023; Thanh et al., 2025). These findings are in line with previous studies, which show that synthetic polymers can alter the chemistry at the nanoparticle/biogenic coating agent interface without completely replacing it.

The most significant and relevant result for the application is the evaluation of UV protection capacity. Gold particles without PVA are more effective in preventing UV exposure, especially during mid-storage, with high SPF values (Thanh et al., 2025). This unconventional behavior provides convincing evidence of the functional optimum that favors nano particle aggregation as a means of maximizing UV scattering and absorption efficacy. The partial aggregation process has been shown to have a dual impact on the effective optical cross-section and plasmonic coupling between particles. This, in turn, has been shown to enhance interactions with UV light, especially UV-B (Pratap & Soni, 2021; Raszewska-Famielec & Flieger, 2022). PVA-stabilized systems, on the other hand, while more colloidally stable, have lower SPF values. UV shielding by the polymer layer, changes in local refractive index, and reduced interparticle coupling effects can be attributed to the disruption of AuNP core-UV interactions.

In summary, our study shows that creating an AuNP system with C. asiatica is not just a matter of design; it must also be considered from an application perspective. The nonlinear relationship between stability (which is enhanced by PVA), aggregation state, and UV protection performance shown here indicates that the assumption that high colloidal stability always results in better properties is no longer true. Instead, it emphasizes that optimization efforts should be directed toward specific functional goals. For UV-protective agents requiring long-term UV protection, systems that can trigger controlled aggregation are superior to maximally stable dispersions. These results provide valuable insights into the design of plant-based nanomaterials and offer a logical framework to guide decision-making between green synthesis conditions, colloidal stability, and functional durability in ecological applications.

CONCLUSION

A green approach was used to synthesize gold nanoparticles, with Centella asiatica extract acting as reducing and capping agents. The addition of poly(vinyl alcohol) led to significant changes in nanoparticle growth dynamics,

as revealed by comprehensive characterization. These changes resulted in larger hydrodynamic sizes and increased colloidal stability due to steric effects. However, this did not result in improved UV-protective performance. AuNP formulations devoid of PVA have been observed to manifest elevated Sun Protection Factor values, thereby signifying the existence of an optimal functional window concomitant with regulated aggregation. These findings show that gold nanoparticle systems made in the lab have a relationship between how stable they are and how useful they are. This shows that it is important to balance these things when designing green, useful nanomaterials.

PRATICAL IMPLICATIONS

The results of this research present valuable practical implications on the development for green-synthesis gold nanoparticle (AuNP) systems studied here in a functional aspect. Upon comparison with previous studies, it is clearly shown that greater colloidal stability adopted by polymeric stabilization such as poly(*vinyl alcohol*), does not always relate to better practical performance in UV-protection applications. It demonstrates the requirement for application based optimization strategies for balancing stability and functional efficacy of the nanoparticles rather than being driven by stability. For the sustainable introduction of nanomaterials in cosmetic and biomedical formulations, however, controlled aggregation states may actually serve a promising way to maximize functional performance according to this study. As a result, the formulation approach should take into account both physicochemical stability and performance-related demands to reach an ideal functionality of material.

LIMITATIONS

However, there are limitations to this study that need to be addressed. This study is limited to optical stability and UV protection performance without considering other functions such as bioactivity or long-term behavior. Second, the range of PVA concentrations and extract compositions studied here is limited, which may restrict the general applicability of the trends observed to other polymer systems or phytochemical profiles. Furthermore, the mechanistic explanation of the interactions between nanoparticles, polymers, and phytochemicals is based on physicochemical analysis rather than investigation at the molecular level.

FUTURE RESEARCH DIRECTIONS

It is hoped that the newly gained insight using therapeutically active payloads in HSFNGs provides a stepping stone towards exploring other identified, stabilizing small polymers or biopolymer substitutions to identify alternative and more economically feasible sources of phytochemicals for tuning functionality of nanoparticles. Sophisticated analytic methods can be used to try and understand the molecular interactions controlling aggregation and surface action. Furthermore, evaluating the performance of green nanoparticles in commercial formulations and biological or environmental conditions would help us understand their practical application. Long-term stability tests and lifecycle analyses would also be helpful to advance towards truly sustainable, application-oriented nanomaterials.

AUTHOR CONTRIBUTIONS

M.A.P. and O.P.A. were responsible for the conceptualization and study design. M.A.P. and S.D.M. performed the experimental work, data collection and laboratory analysis. M.A.P. and S. were responsible for data interpretation and formal analysis. The initial draft was prepared by M.A.P., with critical revisions and intellectual input from all authors. The final version of the manuscript has been read and approved by all authors, who accept full responsibility for the work.

CONFLICT OF INTEREST

The authors declare that there is no conflict of interest regarding the publication of this article.

DATA AVAILABILITY

The data supporting the findings of this study are available from the corresponding author upon reasonable request. The data are not publicly available due to their inclusion as part of a doctoral research project.

FUNDING

This research received no external funding.

ACKNOWLEDGMENT

The authors gratefully acknowledge the support of the laboratories and academic facilities that enabled the completion of this research. Special appreciation is extended to colleagues and technical staff for their assistance during sample preparation, characterization, and data collection.

ETHICAL STATEMENT

This study did not involve human participants or live animals. Therefore, ethical approval was not required.

REFERENCES

Aktar, S. N., Dash, S. S., Hembram, S., Patre, S. S., Barik, S., Kundu, S., Shah, M. H., Islam, M., Pramanik, K., Hossain, A., & Latef, A. A. H. A. (2025). Oilseed Crops and Phytohormones Under UV Stress BT - Oilseed Crops Under Abiotic Stress: Mitigation Strategies and Future Perspectives (A. A. H. Abdel Latef (ed.); pp. 441–470). Springer Nature Singapore. https://doi.org/10.1007/978-981-96-8346-8_14

Alguno, A. C., Capangpangan, R. Y., Dumancas, G. G., Lubguban, A. A., Malaluan, R. M., & Rivera, R. B. P. (2025). Green Synthesis of Gold Nanoparticles Using Plant Extracts. 2(1), 43–52. https://doi.org/10.1007/978-981-96-6565-5_4

Ali, K., Kumar, S., & Khan, M. F. (2025). A concise review on bioactive pentacyclic triterpenoids of Centella asiatica (Gotu Kola). Discover Chemistry, 2(1), 54. https://doi.org/10.1007/s44371-025-00120-3

Anandan, J., Shanmugam, R., Alharbi, N. S., & Thiruvengadam, M. (2025). Green-synthesized silver nanoparticles from Centella asiatica and Ayapana triplinervis: A novel approach to treating wound infections and reducing antimicrobial resistance. South African Journal of Botany, 177, 617–629. https://doi.org/https://doi.org/10.1016/j.sajb.2024.12.020

Arulnangai, R., Ganesamoorthy, R., Mohamed, V. B. H., Vivekanand, P. A., Kavitha, P., Kavitha, P., & Thirugnanasambandham, K. (2025). Green synthesis of silver nanoparticles from Centella asiatica and its application in photodegradation of methylene blue dye in paper industry effluent. Cleaner Water, 4, 100179. https://doi.org/https://doi.org/10.1016/j.clwat.2025.100179

Buraphaka, H., Kitisripanya, T., Yusakul, G., & Putalun, W. (2024). Impact of UV-A and UV-C radiation to enhance triterpenoids and related gene expression in triterpenoid pathway of Centella asiatica postharvest. Industrial Crops and Products, 214, 118579. https://doi.org/https://doi.org/10.1016/j.indcrop.2024.118579

Das, R. K., Pachapur, V. L., Lonappan, L., Naghdi, M., Pulicharla, R., Maiti, S., Cledon, M., Dalila, L. M. A., Sarma, S. J., & Brar, S. K. (2017). Biological synthesis of metallic nanoparticles: plants, animals and microbial aspects. Nanotechnology for Environmental Engineering, 2(1), 18. https://doi.org/10.1007/s41204-017-0029-4

Dewi, R. L., Yuniati, R., & Yasman. (2025). Utiliization of Natural Compound from Pegagan (Centella asiatica (L.) Urb.) and Their Potential Role in the Health Sector. Jurnal Penelitian Pendidikan IPA, 11(4), 94–103. https://doi.org/10.29303/jppipa.v11i4.10558

Fan, Y., Chen, R., Tang, L., Fu, P., Zhou, J., & Chen, X. (2025). Synthesis and Characterization of Molecularly Imprinted Polymers for the Selective Extraction of Triterpenoid Saponin From Centella asiatica Crude Extracts. Journal of Separation Science, 48(4), e70128. https://doi.org/https://doi.org/10.1002/jssc.70128

Fathi, A., Shiade, S. R. G., Saleem, A., Shohani, F., Fazeli, A., Riaz, A., Zulfiqar, U., Shabaan, M., Ahmed, I., & Rahimi, M. (2025). Reactive Oxygen Species (ROS) and Antioxidant Systems in Enhancing Plant Resilience Against Abiotic Stress. International Journal of Agronomy, 2025(1), 8834883. https://doi.org/https://doi.org/10.1155/ioa/8834883

Fekrirad, Z., Darbouy, M., & Molabashi, Z. A. (2026). Chapter 11 - Oxidative stress and the response of bacteria to it. In A. B. T.-M. S. S. Kumar (Ed.), Developments in Microbiology (pp. 217–238). Academic Press. https://doi.org/https://doi.org/10.1016/B978-0-443-27622-4.00024-9

Fu, L., Huang, Y., Sun, X., Wang, X., Li, S., Wang, X., Kang, Q., Shen, D., & Chen, L. (2025). Reactive oxygen species activatable nanotherapeutics for evaluating and relieving nanoplastics-induced oxidative stress. Chemical Engineering Journal, 524, 169081. https://doi.org/https://doi.org/10.1016/j.cej.2025.169081

Fujii, T., Wakaizumi, M., Ikami, T., & Saito, M. (2008). Amla (Emblica officinalis Gaertn.) extract promotes

procollagen production and inhibits matrix metalloproteinase-1 in human skin fibroblasts. Journal of Ethnopharmacology, 119(1), 53–57. https://doi.org/https://doi.org/10.1016/j.jep.2008.05.039

Haftek, M., Abdayem, R., & Guyonnet-Debersac, P. (2022). Skin Minerals: Key Roles of Inorganic Elements in Skin Physiological Functions. In International Journal of Molecular Sciences (Vol. 23, Issue 11, p. 6267). https://doi.org/10.3390/ijms23116267

Hashim, P. (2011). Centella asiatica in food and beverage applications and its potential antioxidant and neuroprotective effect. International Food Research Journal, 18(4), 1215–1222.

Jangpangi, D., Patni, B., Chandola, V., & Chandra, S. (2025). Medicinal plants in a changing climate: understanding the links between environmental stress and secondary metabolite synthesis. Frontiers in Plant Science, 16(June), 1–15. https://doi.org/10.3389/fpls.2025.1587337

Jiang, J., Han, R., Ren, H., Yao, Y., & Jiang, W. (2025). A review of neuroprotective properties of Centella asiatica (L.) Urb. and its therapeutic effects. Annals of Medicine, 57(1), 2559122. https://doi.org/10.1080/07853890.2025.2559122

Jomova, K., Raptova, R., Alomar, S. Y., Alwasel, S. H., Nepovimova, E., Kuca, K., & Valko, M. (2023). Reactive oxygen species, toxicity, oxidative stress, and antioxidants: chronic diseases and aging. Archives of Toxicology, 97(10), 2499–2574. https://doi.org/10.1007/s00204-023-03562-9

Khatami, M., & Iravani, S. (2021). Green and Eco-Friendly Synthesis of Nanophotocatalysts: An Overview. Comments on Inorganic Chemistry, 41(3), 133–187. https://doi.org/10.1080/02603594.2021.1895127

Khavani, M., Mehranfar, A., & Mofrad, M. R. K. (2024). On the interactions of peptides with gold nanoparticles: effects of sequence and size. Journal of Biomolecular Structure and Dynamics, 42(9), 4429–4441. https://doi.org/10.1080/07391102.2023.2220816

Li, C., Luo, Z., Feng, H., & Li, Z. (2025). Polymers Facilitating Therapeutic Efficacy and Applications for Traditional Chinese Medicine. Journal of Polymer Science, 63(4), 839–863. https://doi.org/https://doi.org/10.1002/pol.20240904

Li, L., Luo, X., Liu, Y., Jiang, Y., Chen, Y., Chen, Y., & Wang, J. (2025). Network Meta-analysis of Randomized Controlled Trials Assessing Neuromodulation Therapies for Painful Diabetic Neuropathy. Neurology and Therapy, 14(4), 1355–1382. https://doi.org/10.1007/s40120-025-00759-1

Linh, T. C., & Duc, C. K. T. (2025). Analytical methods for antioxidant screening of endophytic bacteria: A comparative review. Journal of Microbiological Methods, 237, 107224. https://doi.org/https://doi.org/10.1016/j.mimet.2025.107224

Linima, V. K., Ragunathan, R., & Johney, J. (2024). Biofabrication of Centella asiatica mediated metal (Silver and Iron) nanoparticles and their enhanced antimicrobial, anticancer activity in retinoblastoma Y79 cancer cells. Nano-Structures & Nano-Objects, 39, 101226. https://doi.org/https://doi.org/10.1016/j.nanoso.2024.101226

Lv, X., Lin, A., Cui, X., Li, Y., Guo, Z., Tan, X., & Duan, G. (2025). The Interplay Between Climate Warming Driven by Greenhouse Gas Emissions and the Ecotoxicological Effects of Microplastics: Insights From a Meta-Analysis. Global Change Biology, 31(7), e70348. https://doi.org/https://doi.org/10.1111/gcb.70348

Malik, A. Q., Mir, T. ul G., Kumar, D., Mir, I. A., Rashid, A., Ayoub, M., & Shukla, S. (2023). A review on the green synthesis of nanoparticles, their biological applications, and photocatalytic efficiency against environmental toxins. Environmental Science and Pollution Research, 30(27), 69796–69823. https://doi.org/10.1007/s11356-023-27437-9

Manotham, S., Khieokae, M., & Butnoi, P. (2023). Electrospun biopolymer polyvinyl alcohol/Centella asiatica extract nanofibers for antibacterial activity. Materials Today: Proceedings. https://doi.org/https://doi.org/10.1016/j.matpr.2023.06.166

Mukherjee, P. K., Maity, N., Nema, N. K., & Sarkar, B. K. (2011). Bioactive compounds from natural resources against skin aging. Phytomedicine, 19(1), 64–73. https://doi.org/https://doi.org/10.1016/j.phymed.2011.10.003

Nakra, S., Tripathy, S., & Srivastav, P. P. (2025). Green and Sustainable Extraction of Bioactive Compounds from Centella asiatica leaves using Microwave Pretreatment and Ultrasonication: Kinetics, Process Optimization, and Biological Activity. Food Biophysics, 20(1), 56. https://doi.org/10.1007/s11483-025-09948-9

Noruzi, M. (2015). Biosynthesis of gold nanoparticles using plant extracts. Bioprocess and Biosystems Engineering, 38(1), 1–14. https://doi.org/10.1007/s00449-014-1251-0

Pastorino, P., Elia, A. C., Mossotto, C., Gabetti, A., Maganza, A., Renzi, M., Pizzul, E., Faggio, C., Prearo, M., & Barceló, D. (2025). Potential ecotoxicological effects of global change on organisms inhabiting high-mountain lakes in the Alps. Science of The Total Environment, 975, 179180. https://doi.org/https://doi.org/10.1016/j.scitotenv.2025.179180

Pratap, D., & Soni, S. (2021). Review on the Optical Properties of Nanoparticle Aggregates Towards the Therapeutic Applications. Plasmonics, 16(5), 1495–1513. https://doi.org/10.1007/s11468-021-01443-4

Rakshit, S., Roy, T., Samanta, A., Datta, R., Jana, P. C., & Gupta, K. (2025). Multifunctional Biogenic Copper Oxide Nanoparticles: A Comprehensive Review on Biomedical Applications, Photocatalytic Wastewater Treatment, and Future Perspective. ChemistrySelect, 10(43), e00809. https://doi.org/https://doi.org/10.1002/slct.202500809

Raszewska-Famielec, M., & Flieger, J. (2022). Nanoparticles for Topical Application in the Treatment of Skin Dysfunctions—An Overview of Dermo-Cosmetic and Dermatological Products. In International Journal of Molecular Sciences (Vol. 23, Issue 24, p. 15980). https://doi.org/10.3390/ijms232415980

Ruth, F., Soeratri, W., Hariyadi, D. M., Septiana, E., Muttaqien, S. El, Munfadlila, A. W., Sekaringtyas, F. C., & Rosyidah, A. (2024). Gold Nanoparticle Synthesized from Centella asiatica: Emphasis on Optimization, Characterization, Antioxidant, Antiglycation, and Cytotoxicity Effect as an Anti-aging Cosmetic Ingredient. BioNanoScience, 15(1), 45. https://doi.org/10.1007/s12668-024-01713-5

Ryu, D. H., Cho, J. Y., Hamayun, M., Lee, S. H., Cha, H. H., Jung, J. H., & Kim, H.-Y. (2025). Optimizing drying time for Centella asiatica (L.) Urban: metabolomic insights into dehydration effects on primary and secondary metabolites. Chemical and Biological Technologies in Agriculture, 12(1), 26. https://doi.org/10.1186/s40538-025-00745-7

Satpathy, G., Chandra, G. K., Manikandan, E., Mahapatra, D. R., & Umapathy, S. (2020). Pathogenic Escherichia coli (E. coli) detection through tuned nanoparticles enhancement study. Biotechnology Letters, 42(5), 853–863. https://doi.org/10.1007/s10529-020-02835-y

Satpathy, S., Patra, A., Ahirwar, B., & Hussain, M. D. (2020). Process optimization for green synthesis of gold nanoparticles mediated by extract of Hygrophila spinosa T. Anders and their biological applications. Physica E: Low-Dimensional Systems and Nanostructures, 121, 113830. https://doi.org/https://doi.org/10.1016/j.physe.2019.113830

Seevaratnam, V. (2012). A c a d e m i c S c i e n c e s. 4.

Sharma, L. G., SenthilKumar, S., Rangan, L., & Pandey, L. M. (2025). Modulation of thermomechanical-induced albumin aggregation by extracts of Centella asiatica. Biochimica et Biophysica Acta (BBA) - Proteins and Proteomics, 1873(5), 141088. https://doi.org/https://doi.org/10.1016/j.bbapap.2025.141088

Shin, Y. K., & Lee, J. G. (2025). Effects of light intensity and temperature on growth and secondary metabolite production of Centella asiatica in vertical farms. Horticulture, Environment, and Biotechnology, 66(6), 1437–1456. https://doi.org/10.1007/s13580-025-00755-2

Sobi, M. A., Usha, D., Rajagopal, R., Arokiyaraj, S., & Bindhu, M. R. (2024). Phytosynthesizing gold nanoparticles: Characterization, bioactivity, and catalysis evaluation. Journal of Molecular Structure, 1302, 137308. https://doi.org/https://doi.org/10.1016/j.molstruc.2023.137308

Soto, K. M., López-Romero, J. M., Mendoza, S., Peza-Ledesma, C., Rivera-Muñoz, E. M., Velazquez-Castillo, R. R., Pineda-Piñón, J., Méndez-Lozano, N., & Manzano-Ramírez, A. (2023). Rapid and facile synthesis of gold nanoparticles with two Mexican medicinal plants and a comparison with traditional chemical synthesis. Materials Chemistry and Physics, 295, 127109. https://doi.org/https://doi.org/10.1016/j.matchemphys.2022.127109

Subathra, M., Shila, S., Devi, M. A., & Panneerselvam, C. (2005). Emerging role of Centella asiatica in improving age-related neurological antioxidant status. Experimental Gerontology, 40(8), 707–715. https://doi.org/https://doi.org/10.1016/j.exger.2005.06.001

Sucharitakul, T., Chatkul, P., Satianrapapong, W., Arinno, A., Wachiradejkul, W., Kittayaruksakul, S., Kwanthongdee, J., Chatree, S., Chatsirisupachai, A., & Pongkorpsakol, P. (2025). Centella asiatica phytochemical Madecassoside enhances skin wound healing and protects against UVB-induced keratinocyte damage. Tissue Barriers, 2532229. https://doi.org/10.1080/21688370.2025.2532229

Suvedi, D., Kumar, A., Kalia, S., Kumar, A., Koul, S., James, A., Kumar, D., Nagraik, R., & Gulilat, H. (2025). Aging and Herbal Interventions: Mechanistic Insights and Therapeutic Potential. Journal of Cosmetic Dermatology, 24(7), e70335. https://doi.org/https://doi.org/10.1111/jocd.70335

Thanayutsiri, T., Patrojanasophon, P., Opanasopit, P., Ngawhirunpat, T., Plianwong, S., & Rojanarata, T. (2020). Rapid synthesis of chitosan-capped gold nanoparticles for analytical application and facile recovery of gold from laboratory waste. Carbohydrate Polymers, 250, 116983. https://doi.org/https://doi.org/10.1016/j.carbpol.2020.116983

Thanh, N. Q., Mai, D. H., Le, T. P. A., Do, N. H. N., & Le, P. K. (2025). Novel chitosan/polyvinyl alcohol gel encapsulating ethanolic Centella asiatica extract for cosmeceutical applications. Polymer Bulletin, 82(2), 523–541. https://doi.org/10.1007/s00289-024-05543-z

Tripathy, S., & Srivastav, P. P. (2023a). Effect of dielectric barrier discharge (DBD) cold plasma-activated water pre-treatment on the drying properties, kinetic parameters, and physicochemical and functional properties of Centella asiatica leaves. Chemosphere, 332, 138901. https://doi.org/https://doi.org/10.1016/j.chemosphere.2023.138901

Tripathy, S., & Srivastav, P. P. (2023b). Encapsulation of Centella asiatica leaf extract in liposome: Study on structural stability, degradation kinetics and fate of bioactive compounds during storage. Food Chemistry Advances, 2, 100202. https://doi.org/https://doi.org/10.1016/j.focha.2023.100202

Wang, L., Hasanzadeh Kafshgari, M., & Meunier, M. (2020). Optical Properties and Applications of Plasmonic-Metal Nanoparticles. Advanced Functional Materials, 30(51), 2005400. https://doi.org/https://doi.org/10.1002/adfm.202005400

Zhou, P., Yang, P., Zhang, K., Guo, H., Du, J., Huang, L., Jin, D., Alolga, R. N., Wang, H., Li, J., Li, P., & Lu, X. (2025). Discovery and engineering of the asiaticoside, madecassoside and asiaticoside B biosynthetic pathway. Plant Physiology and Biochemistry, 223, 109864. https://doi.org/https://doi.org/10.1016/j.plaphy.2025.109864.

